Coronary Angiography

Three-Dimensional Gadolinium-Enhanced Coronary Magnetic Resonance Angiography: Initial Experience

Jie Zheng, Debiao Li, Kyongtae T. Bae, Pamela Woodard, and E. Mark Haacke

Mallinckrodt Institute of Radiology, Washington University Medical School, St. Louis, Missouri

ABSTRACT

We present our initial experience on first-pass gadolinium-enhanced coronary artery magnetic resonance angiography (MRA). Three-dimensional segmented gradient-echo sequences were developed to image coronary arteries within a single breathhold during the injection of a double-dose contrast agent. Comparisons were made between a short TR of 2.7-msec (n = 5) and a long TR of 5.0-msec (n = 3) sequences in terms of the signal-to-noise ratio (SNR) and contrast-to-noise ratio (CNR). An in-plane resolution of roughly 1 × 1 mm² was achieved. Dramatic vascular signal enhancement by a factor of 3–5 was obtained in volunteers following the contrast agent injection, allowing for clear visualization of proximal coronary arteries. The longer TR scans generally performed better in terms of SNR and CNR improvement (approximately 50%) but allowed for less coverage. These preliminary results suggest that gadolinium-enhanced MRA is a useful tool to study proximal coronary arteries with breathhold, but for a larger coverage, a multiple dose approach may be necessary.
KEY WORDS: Contrast agents; Coronary artery; MR angiography.

INTRODUCTION

Coronary artery disease is the major cause of death in industrialized nations. Conventional x-ray coronary angiography has been considered the gold standard to diagnose the presence and determine the severity of coronary artery disease. This technique, however, only determines the morphological appearance of coronary artery struc-ture and has a limited role in assessing the physiological significance of the disease. It is also an invasive and expensive procedure associated with certain risks of morbidity and mortality. In recent years, significant progress has been made in imaging coronary arteries using magnetic resonance (MR) imaging techniques (1–8). This imaging procedure can potentially provide both anatomic and physiological information in the same study session

33

www.dekker.com

and appears promising in certain clinical applications as a noninvasive alternative to cardiac catheterization and x-ray angiography.

The challenge in obtaining high-quality coronary artery images using MR imaging comes from several factors, including cardiac and respiratory motion, the small size of coronary arteries, the highly tortuous course of the vessels, and their adjacency to fat and cardiac chambers. Early clinical studies of MR coronary artery imaging used two-dimensional (2D) techniques (1–3,5–7). Electrocardiogram (ECG) triggering and breathhold were used to minimize cardiac and respiratory motion effects. However, there are several problems associated with 2D methods, including inconsistent breathhold positions, leading to misregistration of adjacent slices acquired from separate breathholds, and partial volume effects due to thick slices. These problems impeded the visualization of coronary arteries and the detection of coronary artery stenosis.

Three-dimensional (3D) imaging techniques can potentially overcome these problems by providing volumetric coverage of the heart with thin slices (8–10). Coronary arteries can then be viewed from any angle by multiplanar reconstruction. Nevertheless, to collect a 3D scan within a single breathhold, the repetition time (TR) of the pulse sequence has to be reduced dramatically, resulting in a high signal bandwidth and a low signal-to-noise ratio (SNR). A T1-shortening contrast agent may help improve the SNR of MR coronary angiography (11). This approach has been successfully used in improving the SNR of carotid (12), pulmonary (13), abdominal (14,15), and peripheral (16) MR angiography (MRA). In this report, we present our initial experience on 3D breathhold coronary artery imaging with gadolinium-based contrast agent and address the practical issues of data acquisition timing and sequence parameter optimization.

MATERIALS AND METHODS

Dynamic Blood T1 Measurement

The optimal choices of sequence parameters for contrast-enhanced coronary artery imaging, such as the flip angle and TR, depend on the T1 of blood in the presence of contrast agents. To dynamically measure the arterial blood T1 after contrast agent injection, a 2D ultrafast gradient-echo sequence (TR 2.4 msec, data acquisition matrix 64 × 128, flip angle 20°) with a 90° preparatory pulse was used to acquire images at the level below the

aortic arch. To minimize inflow effect on the blood signal, ECG triggering was used to ensure that the images were acquired during diastole when arterial blood flow is relatively slow and constant. Signal intensity of the images can be calculated as follows:

$$S_n = S_0 \left[(1 - e^{TR/T1}) \frac{1 - \cos^{n-1}\alpha \ e^{-(n-1)TR/T1}}{1 - \cos\alpha \ e^{TR/T1}} + \cos^{n-1}\alpha \ e^{-(n-1)TR/T1}(1 - e^{TI/T1}) \right] \sin\alpha \quad (1)$$

where S_0 is a scale factor, n is the number of excitation radiofrequency pulses applied before the collection of the central k-space line, and TI is the time delay from the 90° pulse to the start of the data acquisition. Signal decay caused by T2* is neglected because of the extremely short TE used (TE 1.2 msec).

First, a precontrast image was acquired with a TI of approximately 1000 msec. The T1 of precontrast blood is assumed to be 1200 msec. The purpose of the precontrast scan was to calculate the scale factor S_0 using Eq. (1). The postcontrast images were then collected consecutively, with a temporal resolution of one image per heartbeat, immediately after the start of contrast agent injection. The TI of postcontrast data acquisition was reduced to 10 msec because of the dramatically shortened blood T1. With known S_0 and TI, the MR signal intensities measured from the aorta could be transformed to T1 values by using Eq. (1).

To gain knowledge about the blood T1 profile as a function of the contrast agent injection duration, one subject underwent dynamic imaging twice using the T1 measurement protocol described above. A 35-ml gadolinium contrast agent (Omniscan, Nycomed, New York, NY or Magnevist, Berlex, Wayne, NJ) was infused over a period of 20 and 40 sec, respectively, in the two studies. The contrast material was administrated by hand through a 22-gauge intravenous catheter in the antecubital fossa.

Determination of Imaging Start Time

It is important to match the acquisition of the center of k-space to the maximal arterial enhancement (17) in first-pass contrast-enhanced studies. Therefore, it is crucial to estimate the transit time of the contrast agent from the injection site to the coronary arteries, which varies for each individual. Because the central k-space line is collected at the middle of the data acquisition period in our 3D sequence, the delay time between the start of intravenous injection of the contrast agent and start of image acquisition (TD) was determined by (17)

$$TD = TP_{full} - TA \div 2$$
$$TP_{full} = TP_{test} + TF \div 2 \qquad (2)$$

where TP_{full} and TP_{test} are the time intervals from the start of injection to peak arterial enhancement for the full dose and test bolus injections, respectively; TF is the injection time of the full-dose contrast agent; and TA is the data acquisition time. The scheme of determining TD is illustrated in Fig. 1.

To determine TP_{test}, a series of images were collected immediately after the test bolus injection using the sequence for the dynamic T1 measurement with a temporal resolution of one image per second. The transverse slice was placed below the aortic arch, showing both the descending and ascending aorta. A curve of signal intensity
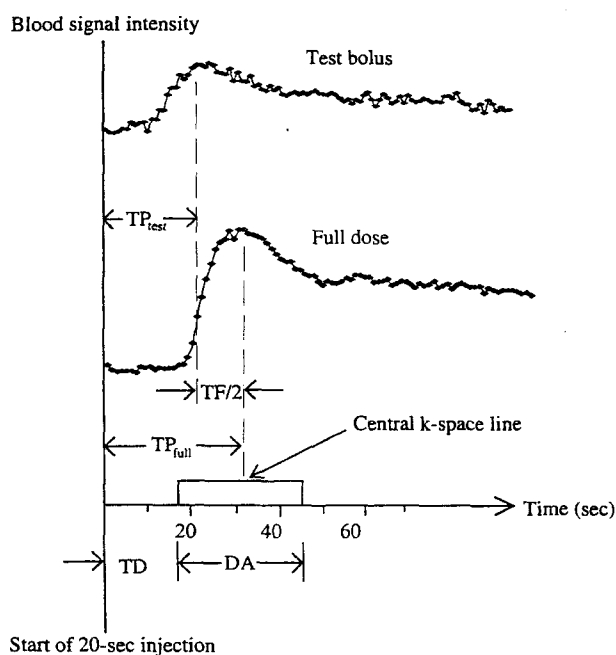
Blood signal intensity

Figure 1. Scheme to determine timing of data acquisition with respect to start of contrast material injection. The blood signal intensity curves are actual data acquired from one subject. See text and Eq. (2) for the definition of various terms. The contrast arrival time of the test bolus appeared slightly faster (2–3 sec) than that of the full dose. The bolus of saline flushed with the test-bolus injection has a greater effect on shortening the circulation time than that with the full-dose injection because of relatively larger saline-to-contrast agent ratio. Other contributing factors would include the discrepancy in contrast volumes between the test dose and full dose that potentially affects maintaining consistent injection rate performed by manual injection.

versus time was then plotted for a region of interest (ROI) placed within the aorta to determine TP_{test}.

Imaging Techniques

The basic structure of the imaging technique is a 3D gradient-echo sequence with segmented in-plane k-space acquisition. To evaluate the SNR of coronary artery images as a function of TR, two versions of the sequence were used. One sequence took advantage of a three-axis gradient overdrive system to achieve a short TR of 2.7 msec. The other sequence used a conventional gradient system and a larger TR of 5.0 msec. In each cardiac cycle, data acquisition occurred in mid diastole for a period of approximately 125 msec, during which 45 and 25 phase-encoding lines were acquired with the short-TR and long-TR sequences, respectively. All 3D slabs were acquired in the transverse orientation. The thickness of the slab was 30–40 mm for the short-TR sequence and 15–20 mm for the long-TR sequence. The field of view was 104 × 260 mm² (phase encoding × frequency encoding). Other sequence parameters are shown in Table 1.

A series of 30 preparatory pulses and a fat saturation pulse were applied before data acquisition during each cardiac cycle. The purpose of the preparatory pulses was to force the myocardial magnetization to reach a steady state. This led to suppression of the myocardial signal when a large flip angle was used.

A typical imaging session consists of the following steps: scout imaging to locate the roots of the left and right coronary arteries, precontrast 3D breathhold coronary MRA in the transverse plane to cover the proximal portions of both left and right coronary arteries, test bolus imaging to determine the appropriate delay time between the start of intravenous injection of contrast material and start of image acquisition, and postcontrast 3D breathhold coronary MRA.

Two subjects were also imaged by a 3D sequence with retrospective respiratory gating (8) (TR/TE 8.0/2.7 msec, bandwidth 244 Hz/pixel, variable flip angles, 16 partitions). The spatial resolution was the same as that of 3D breathhold scans for comparison of image SNR.

Subjects

Eight healthy volunteers (six men, two women, 21–40 years old) underwent gadolinium-enhanced coronary artery imaging. Five subjects were scanned using the short-TR sequence, whereas the other three were scanned using the long-TR sequence. Written informed consent was obtained from each subject before scanning. For ev-

Table 1

Breathhold Coronary MRA Sequence Parameters

TR/Flip Angle	Acquisition Bandwidth (Hz/pixel)	Acquisition Matrix $(N_y \times N_x \times N_z)$	Image Resolution (mm^3) $(\Delta y \times \Delta x \times \Delta z)$	Imaging Time (TA)
2.7/25°	977	90 × 256 × (12–16)	1.2 × 1.0 × 2.5	24–32 heartbeats
5.0/30°	488	100 × 256 × (6–8)	1.0 × 1.0 × 2.5	24–32 heartbeats

N_y, N_x, N_z are the number of points in phase-encoding, frequency-encoding, and 3D partition encoding directions, respectively. Δy, Δx, and Δz are the voxel sizes in the three directions.

ery subject, 35-ml gadolinium contrast agent was injected intravenously by hand over 20 sec, including a 15-ml saline flush immediately after the contrast agent injection. Although it is more customary to administer the contrast agent in a fixed dose per kilogram of body weight, we injected a fixed total amount to each volunteer regardless of body weight (two vials of contrast agents minus 4–5 ml for test bolus). ECG signal was used for triggering the scan, and image data acquisition proceeded during mid diastole with a trigger delay time of 600–900 msec depending on the RR interval of the subject. The subjects were instructed to hold their breath during the scan to eliminate respiratory motion.

All studies were performed on a 1.5-T Siemens VISION system (Siemens AG, Erlangen, Germany). The maximum gradient strength was 25 mT/m and the gradient rise time was 600 sec with the conventional gradient system and 300 sec with a gradient overdrive system. A commercial anterior-posterior, four-element, phased-array surface coil was used for signal reception. However, for all contrast-enhanced studies, only the two anterior elements were used to allow for a small field of view without image warp-around artifacts.

Data Analysis

Multiplanar reconstruction was performed to view coronary arteries at different angles. For each subject, blood signal measurements were performed on pre- and postcontrast images on the left main coronary artery (LM) and right coronary artery (RCA). To measure the SD of noise, an ROI was placed in the air. Using the fact that the SD of the noise is the mean intensity of the background Rayleigh noise divided by 1.25 (18), the blood SNR and the contrast-to-noise ratio (CNR) between blood and myocardium were calculated as follows:

$$SNR = 1.25 \; \frac{\text{blood signal intensity}}{\text{mean intensity of background}}$$

$$CNR = 1.25 \; \frac{\substack{\text{signal difference between} \\ \text{blood and myocardium}}}{\text{mean intensity of background}} \quad (3)$$

RESULTS

Dynamic Blood T1 Measurement

Figure 2 shows the calculated longitudinal relaxation rate (R1) of blood based on an ROI measurement in the aorta after a 20- and a 40-sec contrast agent injection. The T1 values at the peak effect of the 20- and 40-sec injections were calculated to be 38 and 55 msec, respectively. The full-width at half-maximum (FWHM) of the
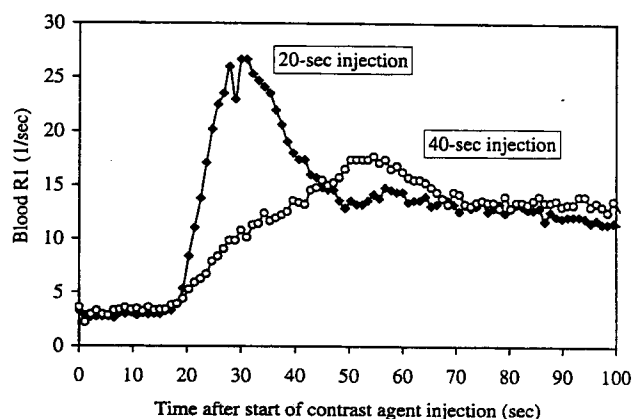

Figure 2. Blood R1 after a 35-ml contrast agent injection with 20- and 40-sec injections for the same subject imaged at different days. Blood T1 at the peak effect for 20- and 40-sec injections are 38 and 55 msec, respectively.
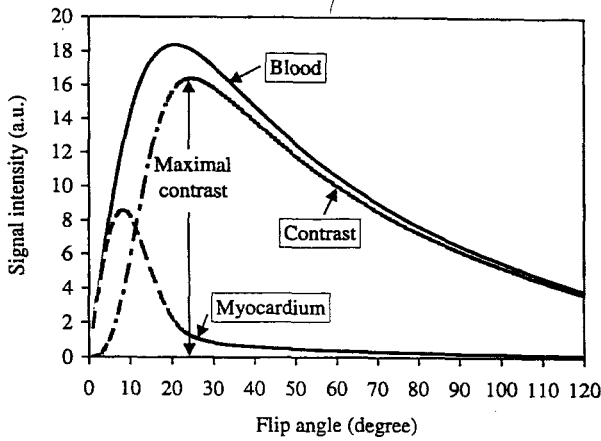
Figure 3. Simulated signal intensities as a function of flip angle for the TR of 2.7-msec gradient-echo sequence with a 20-sec and 35-ml contrast agent injection. It appears that a flip angle of 25° offers maximal contrast between blood (T1 40 msec) and myocardium (T1 800 msec).

20-sec injection is approximately 30 sec, whereas the 40-sec injection has a FWHM of 60 sec. Because the breathhold imaging time was approximately 24–32 sec, a 20-sec injection was chosen for all subjects in the subsequent coronary artery imaging studies because it resulted in a much shorter blood T1.

The flip angle of our 3D gradient-echo sequence was determined by theoretical simulations for the maximal contrast between enhanced arterial blood (T1 ~40 msec) and myocardium (T1 ~800 msec). Figure 3 shows the simulated signal intensities with the short-TR sequence as a function of flip angle. On the basis of this calculation, a flip angle of 25° was chosen for the short-TR sequence and 30° for the long-TR sequence to maximize arterial blood contrast relative to myocardium.

Gadolinium-Enhanced Coronary MRA

In all eight subjects, the LM, the proximal portions of left anterior descending artery (LAD), and RCA were consistently visualized on the postcontrast images. Figure 4 shows typical pre- and postcontrast images obtained using the short-TR sequence. In the precontrast image, both blood and myocardial signals were heavily saturated and no coronary arteries were visible. With contrast agent infusion, blood signals in cardiac chambers and coronary arteries were significantly enhanced, whereas the myocardium remained dark.

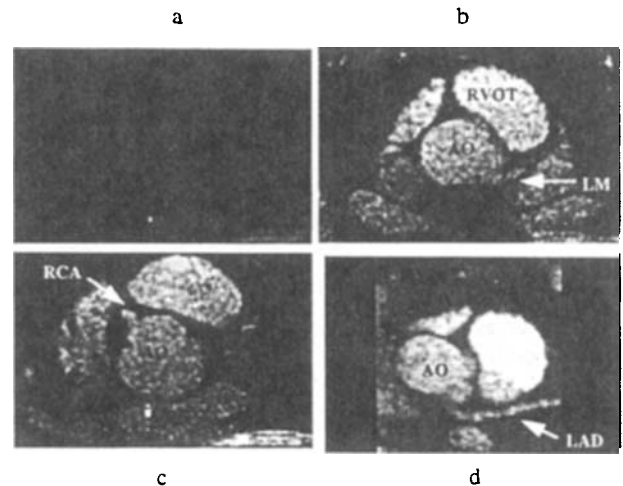Figure 5 illustrates a maximal intensity projection im-

Figure 4. 3D transversal images acquired by the TR 2.7-msec sequence. No coronary arteries are visible in the precontrast image (a) because all tissues are heavily saturated because of the use of the short TR and relatively large flip angle. In postcontrast images (b and c), the LM (b) and the root of RCA (c) are clearly visible. By performing multiplanar reconstruction on the postcontrast 3D data set, a relatively long portion of the proximal LAD is delineated (d). AO, aorta; RVOT, right ventricular outflow tract.

age created from the postcontrast 3D dataset using the long-TR sequence. This image shows well-enhanced LM, LAD, left circumflex, and a small portion of the diagonal branch. Figure 6 compares images acquired using the short-TR and long-TR sequences on two subjects, respectively. Clearly, the SNR of the LM in the long-TR image
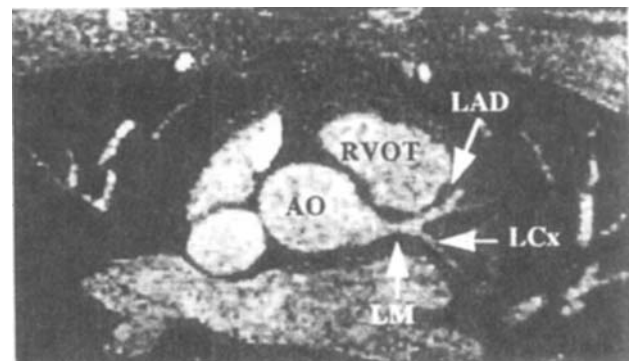

Figure 5. Maximum intensity projection image created from a postcontrast 3D dataset obtained using the TR 5.0-msec sequence. Marked enhancement of the LM, LAD, and left circumflex (LCx) are clearly shown.
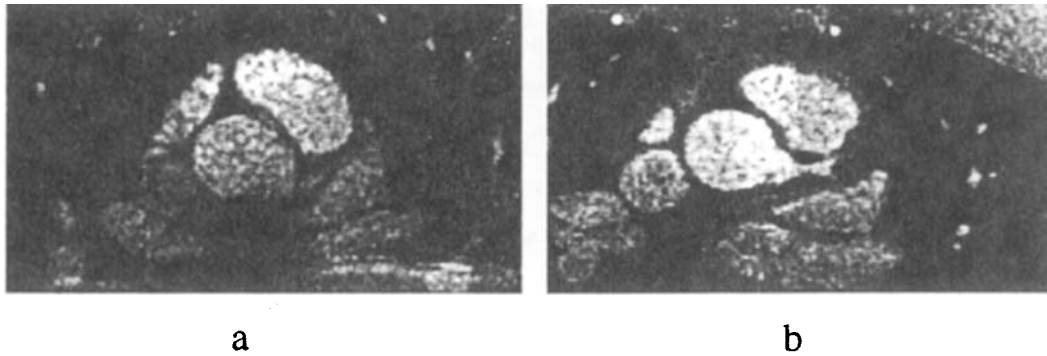
a   b

Figure 6. Comparison between images acquired by the short-TR (a) and long-TR (b) sequences. SNR of LM is 3.4 on (a) and 5.6 on (b).

[Fig. 6(b)] is substantially higher than that in the short-TR image [Fig. 6(a)].

The SNR and CNR of contrast-enhanced coronary arteries measured from the eight subjects are shown in Fig. 7. Compared with precontrast, postcontrast images show a 300–500% improvement in SNR and CNR. Both SNR and CNR of coronary vessels imaged by the long-TR sequence are approximately 50% higher than those imaged by the short-TR sequence ($p < 0.05$).

In Fig. 8, images acquired using contrast-enhanced 3D breathhold MRA sequences are compared with those obtained using the 3D retrospective respiratory gating sequence. High-quality coronary artery images were obtained using the respiratory gated sequence [Fig. 8(a) and (c)], but the acquisition time was long (over 8 min). The short-TR breathhold image [Fig. 8(b)] had a substantially lower SNR (4.9) in the RCA than the respiratory gated image [SNR 9.4, Fig. 8(a)]. On the other hand, the long-TR breathhold image [Fig. 8(d)] had a similar SNR (6.7) as the respiratory gated image [SNR 7.8, Fig. 8(c)] in the LM. Nevertheless, both breathhold images have higher CNR than the respiratory gated images because the myocardial signal was suppressed in contrast-enhanced breathhold scans.
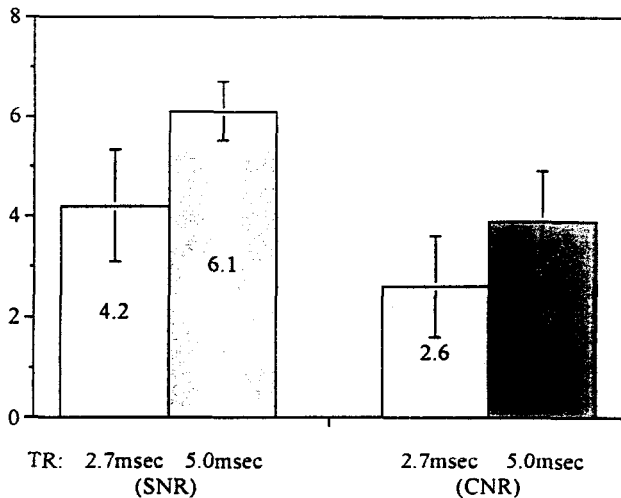

TR: 2.7msec   5.0msec   2.7msec   5.0msec
          (SNR)   (CNR)

Figure 7. Comparison of the coronary artery SNR (a) and CNR (b) obtained using the two sequences of different TRs with contrast agents.

a   b
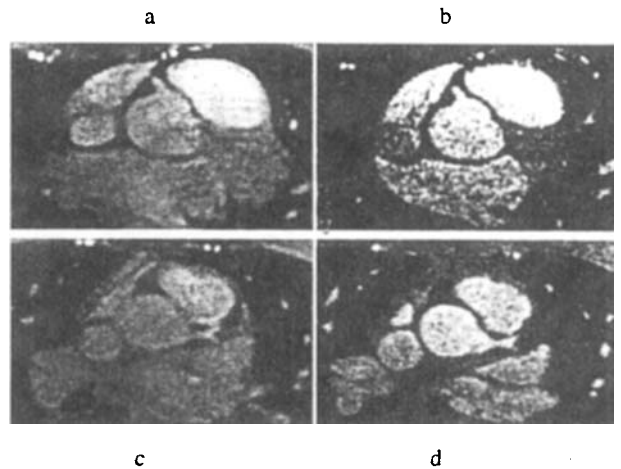
c   d

Figure 8. Comparison of retrospective respiratory gated images without contrast agent (a and c) and gadolinium-enhanced breathhold images acquired with the short-TR sequence (b) and the long-TR sequence (d).

DISCUSSION

A major challenge in coronary artery imaging using MR imaging has been to account for respiratory motion. The respiratory gated techniques (7,8,10,19) are patient friendly but usually require a regular breathing pattern and a rather long imaging time (5–10 min per 3D scan). Breathhold can, in principle, completely eliminate respiratory motion artifacts (9,11,20,21). However, spatial resolution and volume coverage in a 3D breathhold scan could be limited because of the short imaging time. Reducing TR is one way to increase the number of phase-encoding lines per cardiac cycle, thus increasing the spatial resolution, but the SNR will be reduced accordingly. Moreover, with 3D imaging, spin saturation effects may further reduce blood signal, particularly for slow blood flow and short TR.

An initial attempt of 3D breathhold coronary MRA during the first pass of gadolinium injection has been reported recently (11). With markedly reduced T1 of blood, the SNR of coronary arteries increased by a factor of 4 to 5. Because the blood signal on contrast-enhanced MRA relies mainly on the T1 shortening effect instead of the inflow effect, imaging volume could be oriented along any desired direction to cover vessels of interest without the saturation problems associated with time-of-flight MRA.

In this article, several issues are addressed to further improve 3D breathhold contrast-enhanced MRA of coronary arteries: a systemic investigation of the dynamic change of blood T1 during the first-pass of gadolinium injection, the evaluation of the time-to-peak enhancement after a test bolus and full-dose contrast agent injection in the same subject, the use of segmented in-plane phase encoding strategy to improve in-plane resolution to approximately 1×1 mm^2, and the comparison of the image SNR and CNR obtained by using sequences with different TR values.

Our dynamic T1 measurement has a temporal resolution of one image per heartbeat and appears to be consistent with that previously reported (22,23). Although the exact T1 values may vary among different individuals, this measurement, nevertheless, provides a guidance for optimization of flip angles of our imaging sequences.

Based on our experience and the literature (24–26), the appropriate timing of data acquisition with respect to contrast injection is critically important for successful contrast-enhanced MRA. The acquisition of the central k-space should be synchronized to the peak arterial concentration of the contrast agent to achieve maximal blood

signal enhancement. The time from injection to peak enhancement needs to be determined for each subject because it depends on individual cardiovascular parameters (cardiac output, total blood volume, etc.). Previous studies investigated this issue with respect to their specific applications, and several methods have been proposed to detect the arrival of contrast material and to trigger data acquisition (24,25,27). We currently used the peak time for the test bolus to predict for a full dose. A theoretical model and computed tomography studies (28) demonstrated that the peak time of a full-dose injection is delayed approximately half of the infusion time from the peak time of the test bolus, which was verified in our study. This method appears to have worked well in our studies.

The in-plane segmentation strategy allowed us to achieve a higher in-plane resolution (1×1 mm^2) than previous studies (11). The conflict of the high in-plane resolution requirement and the limited gradient capability could be eased. The problem is the small number of partitions and/or relatively long breathhold time per scan. With the long TR sequence, we only acquired six to eight partitions within 24–32 heartbeats. This is a major limitation of the first-pass contrast-enhanced MRA. One way to alleviate this problem is to orient a localized 3D slab along the vessel axis, which may be adequate to cover a major portion of one side of the coronary artery system (29), particularly for the RCA system. However, for the short-TR sequence, oblique scans could not be obtained currently in our system because of the use of the gradient overdrive system in three axes. Thus, only a transverse slab with 12–16 partitions could be acquired, which may be useful to cover left coronary arteries but may not be the appropriate orientation for imaging right coronary arteries. Half Fourier data acquisition (11) may also help improve 3D volume coverage and/or in-plane resolution without increasing the breathhold time.

One aim of our studies was to compare SNR and CNR of images acquired with different TRs. It became clear that even with the help of double-dose contrast agents and data acquisition during first pass, SNR of the coronary arteries in the TR of 2.7-msec sequence is still inferior to that obtained using the retrospective respiratory gated sequence, which has a TR of 8.0 msec and a much lower bandwidth. By using a longer TR and a lower bandwidth, the SNR of the contrast-enhanced scan was improved by about 50% and became comparable with that using the respiratory gated sequence without contrast agent injection. However, the tradeoff of the contrast-enhanced long-TR sequence is the reduced number of

slices available in a breathhold. Moreover, it seems that greater SNR may still be needed for this method to become clinically useful.

An important practical issue in first-pass imaging is that the failure of ECG triggering may cause severe deterioration of image quality. First, some cardiac cycles may be skipped, leading to an increase in data acquisition time. Thus, the collection of the central k-space may not be properly timed to the peak concentration of the contrast agent. Second, subjects may not be able to hold their breath for an unexpected longer acquisition time, and respiratory motion artifacts may occur. This problem needs to be carefully addressed to ensure consistent image quality and blood signal enhancement.

In conclusion, our study suggests that 3D breathhold contrast-enhanced MRA has the potential to become a useful technique for imaging coronary arteries. Further improvement in SNR, resolution, and volume coverage is essential to visualize distal portions of coronary arteries. Optimization of contrast agent injection mode and use of more SNR efficient coils will help improve SNR. Other techniques such as partial Fourier data acquisition (11), simultaneous acquisition of spatial harmonics technique (30), and segmented echo planar acquisition (9,31) will help speed up data acquisition, improve resolution, and increase volume coverage. Finally, intravascular contrast agents offer greater relaxivity and longer data acquisition window and will prove more appropriate for coronary MRA than conventional extravascular contrast agents used in this study.

REFERENCES

1. Edelman RR, Manning WJ, Burstein D and Paulin S. Coronary arteries: Breath-hold MR angiography. *Radiology*, 1991; 181:641–643.
2. Meyer CH, Hu BS, Nishimura DG and Macovski A. Fast spiral coronary artery imaging. *Mag Reson Med*, 1992; 28:202–213.
3. Manning WJ, Li W and Edelman RR. A preliminary report comparing magnetic resonance coronary angiography with conventional angiography. *N Engl J Med*, 1993; 328:828–832.
4. Li D, Pascahal CB, Haacke EM and Adler LP. Coronary arteries: Three-dimensional MR imaging with fat saturation and magnetization transfer contrast. *Radiology*, 1993; 187:401–406.
5. Duerinckx AJ and Urman MK. Two-dimensional coronary MR angiography: Analysis of initial clinical results. *Radiology*, 1994; 193:731–738.
6. Pennell DJ, Bogren HG, Keegan J, Firmin DN and Un-derwood SR. Assessment of coronary artery stenosis by magnetic resonance imaging. *Heart*, 1996; 75:127–133.
7. Oshinski JN, Hofland L, Mukundan S, Dixon WT, Parks WJ and Pettigrew RI. Two-dimensional coronary MR angiography without breath-holding. *Radiology*, 1996; 201: 737–743.
8. Li D, Kaushikkar S, Haacke EM, Woodard PK, Dhawale PJ, Kroeker RM, Laub G, Kuginuki Y and Gutierrez FR. Coronary arteries: Three-dimensional MR imaging with retrospective respiratory gating. *Radiology*, 1996; 201: 857–863.
9. Wielopolski PA, Manning WJ and Edelman RR. Single breath-hold volumetric imaging of the heart using magnetization-prepared 3-dimensional segmented echo planar imaging. *J Magn Reson Imaging*, 1995; 4:403–409.
10. Wang Y, Rossman PJ, Grimm RC, Riederer SJ and Ehman RL. Navigator-echo-based real-time respiratory gating and triggering for reduction of respiratory effects in 3D coronary imaging. *Radiology*, 1996; 198:55–60.
11. Goldfarb JW and Edelman RR. Contrast-enhanced breath-hold 3D coronary magnetic resonance angiography. *Radiology*, 1998; 187:719–722.
12. Kim JK, Farb RI and Wright GA. Test bolus examination in the carotid artery at dynamic gadolinium-enhanced MR angiography. *Radiology*, 1998; 206:283–289.
13. Hatabu H, Jochen G, Kim D, Li W, Prasad PV and Edelman RR. Pulmonary perfusion and angiography: Evaluation with breath-hold enhanced three-dimensional fast imaging steady-state precession MR imaging with short TR and TE. AJR *Am J Roentgenol*, 1996; 167:653–655.
14. Prince MR, Narasimham DL, Stanley JC, et al. Breath-hold gadolinium-enhanced MR angiography of the abdominal aorta and its major branches. *Radiology*, 1995; 197:785–792.
15. Hany TF, Debatin JF, Leung DA and Pfammatter T. Evaluation of the aortoiliac and renal arteries: Comparison of breath-hold, contrast-enhanced, three-dimensional MR angiography with conventional catheter angiography. *Radiology*, 1997; 204:357–362.
16. Adamis MK, Li W, Wielopolski PA, et al. Dynamic contrast-enhanced substraction MR angiography of the lower extremities: Initial evaluation with a multisection two-dimensional time-of-flight sequence. *Radiology*, 1995; 196:689–695.
17. Earls JP, Rofsky NM, DeCorato DR, Krinsky GA and Weinreb JC. Breath-hold single-dose gadolinium-enhanced three-dimensional MR aortography: Usefulness of a timing examination and MR power injector. *Radiology*, 1996; 201:705–710.
18. Henkelman RM. Measurement of signal intensities in the presence of noise in MR images. *Med Phys*, 1985; 12: 232–233.
19. Sachs TS, Meyer CH, Irarrazabal P, Hu BS, Nishimura

DG and Macovski A. The diminishing variance algorithm for real-time reduction of motion artifacts in MRI. *Magn Reson Med,* 1995; 34:412–422.

20. Dolye M, Scheidegger MB, de Graaf RG, Vermeulen J and Pohost GM. Coronary artery imaging in multiple 1-sec breath-holds. *Magn Reson Imaging,* 1993; 11:3–6.

21. Sakuma H, Caputo GR, Steffens JC, O'Sullivan M, Bourne MW, Shimakawa A, Foo TK and Higgins CB. Breath-hold MR cine angiography of coronary arteries in healthy volunteers: Value of multiangle oblique imaging planes. AJR *Am J Roentgenol,* 1994; 163:533–537.

22. Larsson HB, Stubgaard M, Sondergaard L and Henriksen O. In vivo quantification of the unidirectional influx constant for Gd-DTPA diffusion across the myocardial capillaries with MR imaging. *J Magn Reson Imaging,* 1994; 4:433–440.

23. Strouse PJ, Prince MR and Chenevert TL. Effect of the rate of gadopentetate dimeglumine administration on abdominal vascular and soft-tissue MR imaging enhancement patterns. *Radiology,* 1996; 201:809–816.

24. Prince MR, Chenevert TL, Foo TKF, Londy FJ, Ward JS and Maki JH. Contrast-enhanced abdominal angiography: Optimization of imaging delay time by automating the detection of contrast material in the aorta. *Radiology,* 1997; 203:109–114.

25. Hany TF, Mckinnon GC, Leung DA, Pfammatter T and Debatin JF. Optimization of contrast timing for breath-hold three-dimensional MR angiography. *JMRI,* 1997; 7: 551–556.

26. Maki JH, Prince MR, Londy FJ and Chenevert TL. The effects of time varying intravascular signal intensity and k-space acquisition order on three-dimensional MR angiography image quality. *JMRI,* 1996; 6:642–651.

27. Wilman AH, Riederer SJ, King BF, Debbins JP, Rossman PJ and Ehman RL. Fluoroscopically triggered contrast-enhanced three-dimensional MR angiography with elliptical centric view order: Application to the renal arteries. *Radiology,* 1997; 205:137–146.

28. Bae KT, Heiken JP, Li D, Zheng J and Haacke EM. Pharmacokinetic analysis of aortic contrast enhancement timing in Gd-Enhanced MRA. *Proceedings of International Society for Magnetic Resonance in Medicine.* Sydney, Australia, 1998, p. 764.

29. Wielopolski PA, van Geuns RJM, de Feyter PJ, Oudkerk M and den Hoed Kliniek D. VCATS, MR coronary angiography using breath-hold volume targeted acquisitions. *Proceedings of International Society for Magnetic Resonance in Medicine,* 1998, p. 14.

30. Sodickson DK and Manning WJ. Simultaneous acquisition of spatial harmonics.(SMASH): Fast imaging with radiofrequency coil arrays. *Magn Reson Med,* 1997; 38: 591–603.

31. Beck GM, Li D, Zheng J, Haacke EM, Noll TG and Schad LR. Three-dimensional MR coronary angiography with a segmented echo planar imaging sequence and retrospective respiratory gating. *Proceedings of International Society for Magnetic Resonance in Medicine,* 1998, p. 319.